Indian Journal of Chemical Technology
Vol. 27, May 2020, pp. 201-209

Dielectric dispersion and electrical conductivity of amorphous PVP–SiO_2 and PVP–Al_2O_3 polymeric nanodielectric films

Shobhna Choudhary*[,1], Priyanka Dhatarwal[2] & R J Sengwa[2]

[1]CSIR-National Institute of Science Communication and Information Resources, New Delhi 110 012, India

[2]Dielectric Research Laboratory, Department of Physics, Jai Narain Vyas University, Jodhpur 342 005, India

E-mail: shobhnachoudhary@rediffmail.com

Received 12 February 2020; accepted 4 March 2020

The biodegradable hybrid polymer nanocomposite (PNC) films comprising silica (SiO_2) and alumina (Al_2O_3) nanoparticles as inorganic nanofillers and the poly(vinyl pyrrolidone) (PVP) as organic host matrix (i.e., PVP–*x* wt% SiO_2 and PVP–*x* wt% Al_2O_3 for *x* = 0, 1, 3 and 5) have been prepared by aqueous solution-casting method. X-ray diffraction (XRD) study reveals that these nanocomposite materials are highly amorphous. The dielectric spectroscopy of these different nanofiller concentrations PNC films has been carried out in the frequency range from 20 Hz to 1 MHz at a fixed temperature and also for 3 wt% nanofillers containing PNC films with the temperature variation. The results confirm that the complex dielectric permittivity of these hybrid films is influenced by the interfacial polarization in the low frequency range of 20 Hz to 1 kHz, whereas in the high frequency range up to 1 MHz permittivity is mainly governed by the molecular polarization and remains almost independent of the frequency. These SiO_2 and Al_2O_3 nanofillers containing PNC films at fixed temperature display anomalous behaviour of dielectric permittivity and ac electrical conductivity with the increase of nanofiller concentration, but these parameters significantly enhance at low frequencies with the increase of temperature of the films. The electric modulus spectra of Al_2O_3 containing PNC film exhibit relaxation peaks below 100 Hz at higher temperatures which attribute to the interfacial polarization relaxation process. The frequency independent dielectric permittivity and significantly low loss of these PNC materials at radio frequencies confirm their suitability as polymeric nanodielectric (PND) substrate and insulator in the design and fabrication of biodegradable electronic devices and electrical components.

Keywords: Polymer nanocomposite, Nanodielectrics, Dielectric properties, Electrical conductivity, XRD, Dielectric spectroscopy

Owing to the rapid growth of flexible-type microelectronic and optoelectronic devices based on modern polymer technology, the demand for suitable dielectrics and insulators promotes the development of a variety of promising properties polymeric nanodielectrics (PNDs)[1–13]. Since the traditional polymeric dielectrics have reached their physicochemical and thermomechanical limits, the research on advanced multifunctional PNC materials based nanodielectrics has become a hot spot in the last decade[1,3,9,12,14,15]. The PNDs are the materials comprising of appropriate properties polymer as a host matrix with homogeneously dispersed organic or inorganic nanomaterial of unique electrical and optical properties which involves nanotechnology[1,3–6,10,11]. These hybrid materials can be used as passive or active dielectrics in the fabrication of new generation flexible microelectronic devices[1,2,8,13–15]. So far, numerous synthetic polymers and a variety of inorganic/organic nanomaterials have been considered for the development of polymer nanocomposites of novel dielectric, electrical, optical, mechanical, thermal, and environmental-friendly properties for their practical applications[1–3,5,6,8–11,13–18].

The polymer nanocomposites based on poly(vinyl pyrrolidone) (PVP) matrix[19–24] and its blend matrices with other polymers[9,15,25–28] have attracted the attention of many researchers for the development of novel multifunctional nanocomposite materials. It has been established that the type of nanofiller and its homogeneous dispersion in the polymer matrix play a significant role in achieving the important properties of the composite materials[1,3,5]. According to the area of interest, different characterization techniques can be considered for the confirmation of useful properties of the PNC materials. The biodegradable and biocompatible PVP is an amorphous polar polymer, and its monomer unit possesses pyrrolidone

ring of carbonyl functional group which exhibits strong affinity to several inorganic/organic nanofillers and therefore along with the use of PVP as host matrix in the preparation of PNCs[19–24], it is frequently used as capping-agent/encapsulator to avoid agglomeration of nanoparticles and reducing the particle sizes in the nanomaterials[29–32].

The studies on numerous PNC materials have established that the nanofiller mostly modifies the chemical and physical properties of the host polymer matrix[1–3,33]. However, several studies have also confirmed that there is huge alteration in the dielectric and electrical properties of a polymer matrix with the addition of nanofiller and change in its loaded amount in the matrix[1,4,5,7,9,14,15,25,34–37]. A variety of non-metal and metal oxides nanomaterials had been used for the preparation of PNCs and confirmation of their suitability as PNDs for the development of flexible type advanced electronic and electrical devices[1,4–10,13,15,16,35–37]. Silica (silicon dioxide; SiO_2) and alumina (aluminium oxide; Al_2O_3) nanomaterials are mostly considered as nanofiller in a host polymer matrix for the development of potential PNDs for the dielectric applications and as electrical insulators, and also their uses in the advances of polymer technology[11,17,18,22,25,38–49].

In this paper, the detailed dielectric and electrical properties of PVP–*x* wt% SiO_2 and PVP–*x* wt% Al_2O_3 nanocomposites have been studied with the variation of frequency, nanofiller concentration, and temperature of the films which have not been attempted yet. The interesting results on these PNCs reveal that they could be used as novel PNDs as substrate and insulator for the development of biodegradable microelectronic devices and numerous other technological uses.

Experimental Section

Materials

The SiO_2 nanopowder of particle sizes in the range 5 to 15 nm (CAS No. 7631-86-9) and the Al_2O_3 nanopowder of particle sizes less than 50 nm (CAS 1344-28-1) of Sigma-Aldrich, USA, and PVP (K_{90}; $M_w \sim 6\times10^5$ g mol^{-1}) fine powder (Product No. 39766) of S D Fine-Chem Limited, Mumbai, India, were used for the preparation of PVP–*x* wt% SiO_2 and PVP–*x* wt% Al_2O_3 films for *x* values 0, 1, 3, and 5 by the facile solution-cast method. For the preparation of each PNC sample, in the beginning, the required amount of PVP was dissolved in deionized water. The amount of SiO_2 or Al_2O_3 for *x* wt% concentration with respect to the weight of PVP was firstly dispersed into the deionized water in a separate glass bottle under magnetic stirring and then it was mixed in the PVP solution. The homogeneous and highly viscous polymeric solution of uniformly suspended nanoparticles was achieved by ultrasonication followed by vigorous magnetic stirring under moderate heating for partial solvent evaporation. The viscous solution so obtained was cast on to poly propylene dish and allowed to dry at room temperature. It was noted that during the process of solution drying, the loaded nanoparticles of nanofiller remained uniformly distributed over the entire volume and height of the casted solution, and there was no sedimentation and agglomeration of the nanoparticles which confirmed the successful formation of the nanocomposite film. All the PNC films with SiO_2 and Al_2O_3 nanofillers of different concentrations *x* (wt%) were prepared by following the same steps given above. The thicknesses of these solution cast free-standing PNC films were found in the range 0.19 to 0.24 mm. These films were further vacuum dried in order to remove the solvent traces if any.

Measurements

The amorphous structure of these nanocomposite materials was characterized by X-ray diffraction (XRD) measurements using a PANalytical X′pert Pro multipurpose diffractometer operated at 1800 W (45 kV and 40 mA). The XRD pattern of each film was recorded at a scan rate of 0.05°/s for better precision. The complex dielectric permittivity over the frequency range from 20 Hz to 1 MHz is determined using precision LCR meter (Agilent technologies 4284A equipped with the 16451B solid dielectric test fixture and microprocessor controlled oven for controlling the temperature of the film under study). The alternating current (ac) electrical conductivity and electric modulus spectra of the PNC films were derived using their frequency dependent dielectric permittivity values. The details of dielectric and electrical measurements are described elsewhere[9].

Results and Discussion

XRD spectra of PNC films

Figure 1 illustrates the XRD patterns of the PVP–*x* wt% SiO_2 and PVP–*x* wt% Al_2O_3 films and also that of the SiO_2 and Al_2O_3 nanopowders. A broad and diffused peak exhibited around 23° confirms the amorphous structure of SiO_2 (see Fig. 1a)[17,25], whereas the characteristic diffraction peaks appeared

at 32.6°, 37.2°, 39.5°, 45.5°, and 67.1° evidence the γ-phase of the Al_2O_3 (see Fig. 1b)[40,41,43]. The pristine PVP film has the characteristic diffused halos at 11.5° and 21° which reveal its highly amorphous structure[28]. The XRD patterns of different SiO_2 concentration PNC films shown in Fig. 1a seem almost identical to that of the pristine PVP film which also confirms their amorphous structures. Similarly, Fig. 1b reveals that there is no change in the shape of the XRD patterns of PVP–*x* wt% Al_2O_3 films with initial 1 wt% loading of Al_2O_3 and also on an increase of its content suggesting that these PNC materials are also predominantly amorphous.

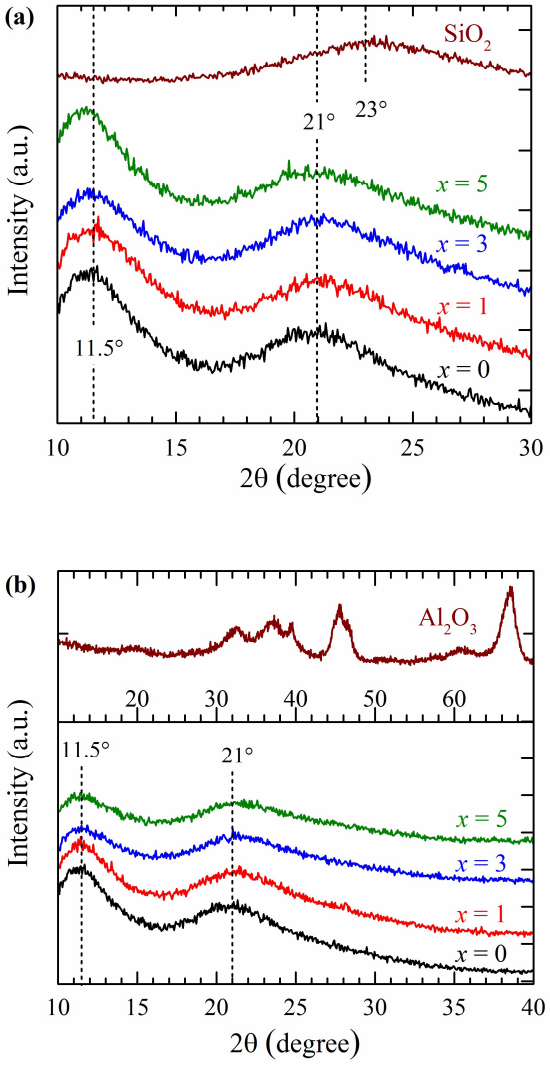

Fig. 1 — The XRD patterns of the (a) PVP–*x* wt% SiO_2 films, and (b) PVP–*x* wt% Al_2O_3 films for *x* values 0, 1, 3 and 5 and also of SiO_2 and Al_2O_3 nanopowders.

Complex dielectric permittivity spectra

The frequency dependence of complex dielectric permittivity (real part ε′ and imaginary part ε″) and dielectric loss tangent (tanδ = ε″/ε′) of the PVP–*x* wt% SiO_2 and PVP–*x* wt% Al_2O_3 films are depicted in Figs. 2 and 3, respectively. These figures illustrate that the ε′, ε″, and tanδ values of both types of PNC films at 30 °C gradually decrease with the increase of frequency from 20 Hz to 1 kHz and thereafter the variation in these values is insignificant up to 1 MHz. The increase of dielectric functions at low frequencies for these materials evidences the contribution of interfacial polarization and it is not effective at high frequencies which attributed to the dipolar polarization (i.e., molecular polarization (MP)). These dielectric results are in agreement with numerous other PNC materials[8,9,15,25,34,39,50–52].

Figure 2 reveals that the ε′ values of these PNC films anomalously change with the increase of SiO_2 content at a fixed frequency and a constant temperature. The spectra of Al_2O_3 containing PNC films (Fig. 3a) also reveal that the ε′ values anomalously vary with the increase of Al_2O_3 contents but they remain always higher than that of the pristine PVP film which is not the case for the SiO_2 containing PNC films. This may be because of the fact that the Al_2O_3 has high permittivity (ε′ = 9.7 at 1 MHz and 30°C)[42,43] as compared to that of the SiO_2 (ε′ = 3.8 at 1 MHz and 27 °C)[11,25]. Further, the ε′ value of SiO_2 is close to that of the pristine PVP (~2.2 at 1 MHz and 30°C as shown in Fig. 2), and therefore the observed ε′ values of these SiO_2 containing PNC films are observed either slightly lower or higher than that of the PVP film.

The dielectric spectra of the PNC films infer that the ε″ and tanδ values at radio frequencies (RF) $f \geq 20$ kHz are lower than 0.03 and 0.02, respectively for the PVP–*x* wt% SiO_2 films and that of the PVP–*x* wt% Al_2O_3 films (see enlarged view in the insets of Figs. 2 and 3). The appreciably stable ε′ values and significantly low tanδ values confirm the suitability of these materials as low dielectric loss nanodielectric materials for substrates and insulators in the design and development of a variety of biodegradable microelectronic devices[2,9,13–15,27,43].

Figures 2b and 3b demonstrate that there is an appreciable increase of ε′ and ε″ values of these PNC materials at low frequencies (f < 1 kHz) with the increase of temperature of the films but at radio frequencies the increase in these values is relatively

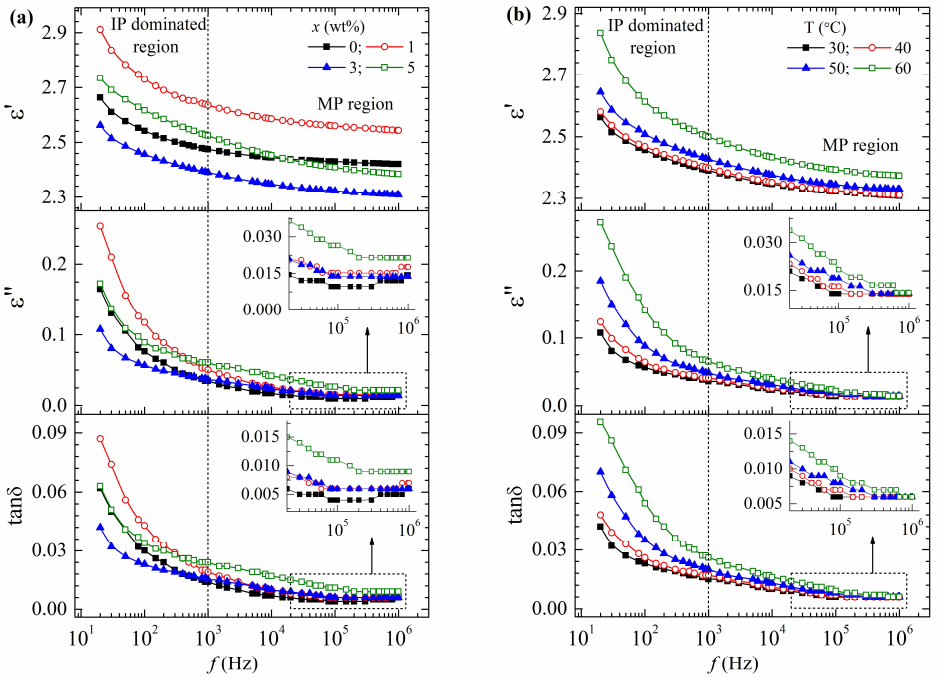

Fig. 2 — The complex dielectric permittivity (real part ε′ and imaginary part ε″) and the loss tangent tanδ spectra of the (a) PVP–*x* wt% SiO_2 films for *x* values 0, 1, 3 and 5 at 30 °C, and (b) PVP–3 wt% SiO_2 film at temperatures 30, 40, 50, and 60 °C. The insets show the enlarged view of ε″ and tanδ at high frequencies.

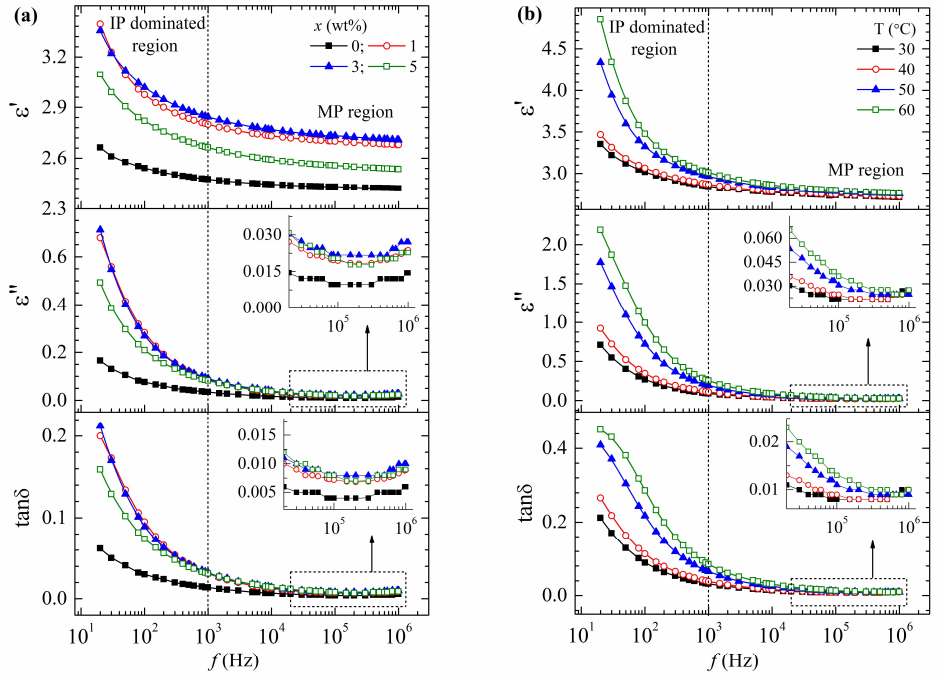

Fig. 3 — The complex dielectric permittivity (real part ε′ and imaginary part ε″) and the loss tangent tanδ spectra of the (a) PVP–*x* wt% Al_2O_3 films for *x* values 0, 1, 3 and 5 at 30 °C, and (b) PVP–3 wt% Al_2O_3 film at temperatures 30, 40, 50, and 60 °C. The insets show the enlarged view of ε″ and tanδ at high frequencies.

insignificant for the Al_2O_3 containing PNC film (see enlarged view given in insets of the figures). This finding infers that the loading of Al_2O_3 nanoparticles stabilizes the dielectric permittivity at radio frequencies relatively better than that of the SiO_2 nanoparticles.

The variation of ε′ and tanδ values as a function of nanofiller concentration x (wt%) for the PVP–x wt% SiO_2 films and PVP–x wt% Al_2O_3 films at a constant temperature, and also as a function of temperature for the 3 wt% nanofillers containing PNC films at 1 kHz and 1 MHz are plotted in Fig. 4. It can be clearly noted from Fig. 4a that the ε′ and tanδ values of both the SiO_2 and Al_2O_3 containing these PNC films

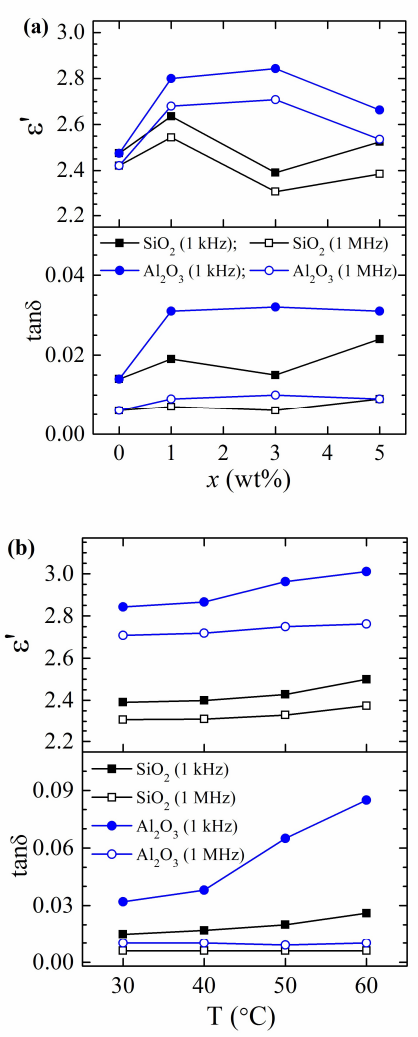

Fig. 4 — The real part ε′ of complex dielectric permittivity and the loss tangent tanδ values at 1 kHz and 1 MHz as a function of (a) nanofiller concentration x (wt%) for the PVP–x wt% SiO_2 films and PVP–x wt% Al_2O_3 films at 30 °C, and (b) temperature for the PVP–3 wt% SiO_2 and PVP–3 wt% Al_2O_3 films.

anomalously vary with the increase of nanofiller contents in the films. Further, at both these frequencies, the ε′ and tanδ values are nearly the same confirming the stability of these dielectric functions over the broad frequency range i.e., from 1 kHz to 1 MHz. Fig. 4b reveals that the ε′ and tanδ values increase non-linearly with the increase of temperature of the PNC films but the rate of increase is relatively high at 1 kHz confirming that the interfacial polarization is relatively more thermally activated as compared to that of the dipolar polarization. The insignificant variation in ε′ and tanδ values at 1 MHz infers that these are thermally stable nanodielectrics over the temperature range 30–60 °C at the higher radio frequencies.

Electric modulus spectra

The electric modulus formalism is frequently considered for analysis of relaxation processes in heterogeneous composite materials because in this formalism the effects of electrode polarization, adsorbed impurities, electrode material, and electrode-dielectric contact etc. get nullified[6,13,15,18,36,37,40,53]. The electric modulus spectra (real part M' and loss part M'') of different PNC films at 30 °C, and also for 3 wt% nanofillers containing PNC films at different temperatures (30–60 °C) are shown in Fig. 5 for SiO_2 nanofiller loaded PNC films and in Fig. 6 for Al_2O_3 containing PNC films. The M' values of these PNC materials exhibit a non-linear increase with the increase of frequency in the low-frequency region but at high frequencies, the increase is relatively small and approaches a steady state near 1 MHz. This type of $M'(f)$ dispersion is a common characteristic for the hybrid composite materials in which M' sharply enhances in the IP-affected low frequency region and exhibit steady state in the dipolar polarization affected high frequency region[9–11,15–18]. Further, the typical dispersion of M' of these heterogeneous PNC films evidence that there is no contribution of the electrode polarization at lower frequencies.

The M'' spectra of these PNC materials show that there is a large decrease of M'' at low frequencies for the SiO_2 containing PNC films (Fig. 5) which is also evidence of the presence of relaxation peak just below 20 Hz corresponding to the interfacial polarization relaxation process. The relaxation peak of this process is observed in 3 wt% Al_2O_3 containing PNC film when it was studied at 50 and 60°C (Fig. 6) which also shows a shift towards higher frequency side with

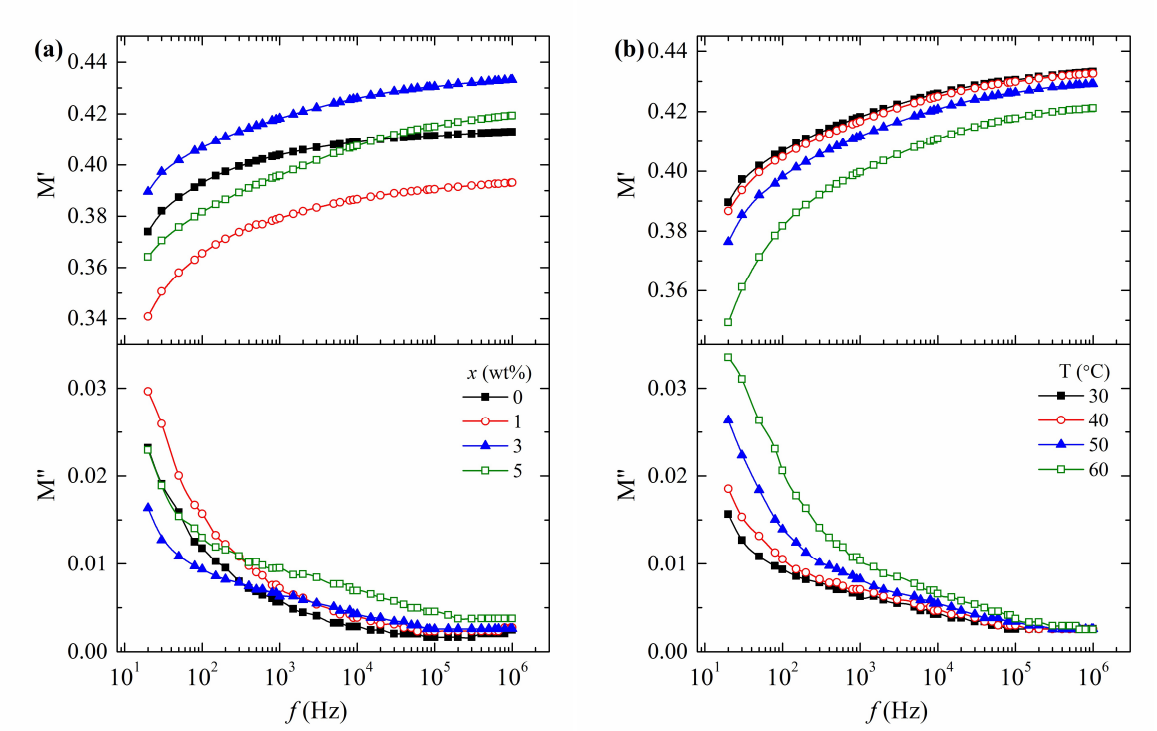

Fig. 5 — Frequency dependent real part M' and loss part M'' of complex electric modulus of the (a) PVP–x wt% SiO_2 films for x values 0, 1, 3 and 5 at 30 °C, and (b) PVP–3 wt% SiO_2 film at temperatures 30, 40, 50, and 60 °C.

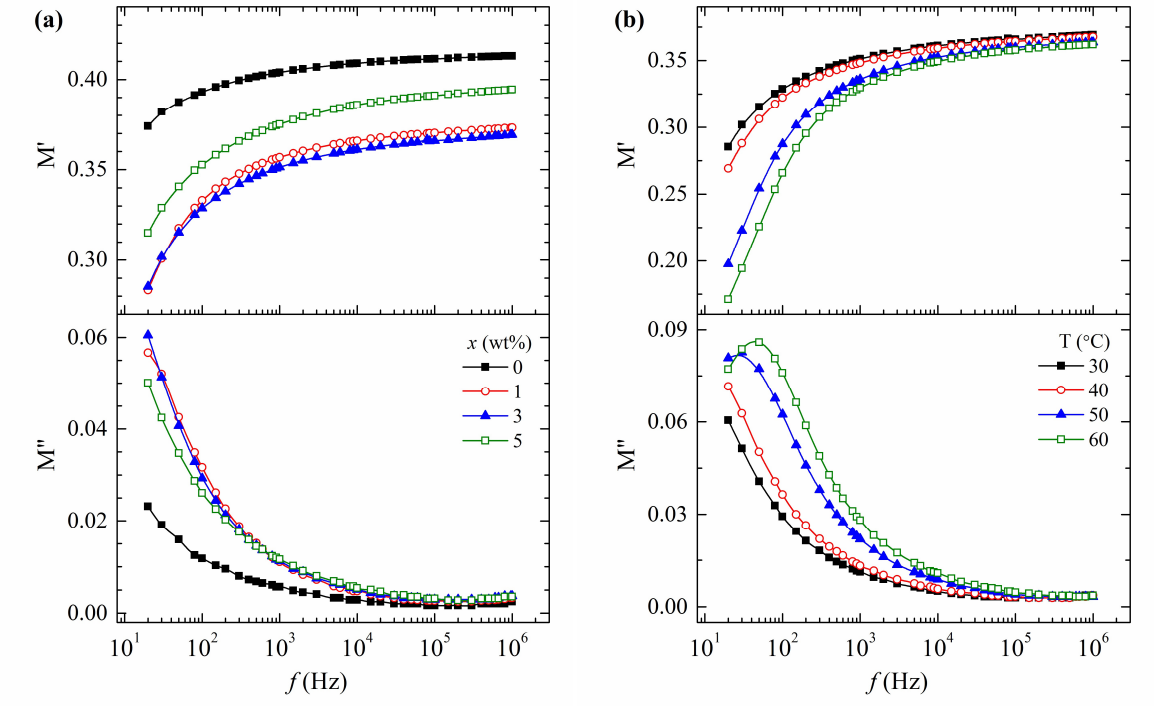

Fig. 6 — Frequency dependent real part M' and loss part M'' of complex electric modulus of the (a) PVP–x wt% Al_2O_3 films for x values 0, 1, 3 and 5 at 30 °C, and (b) PVP–3 wt% Al_2O_3 film at temperatures 30, 40, 50, and 60 °C.

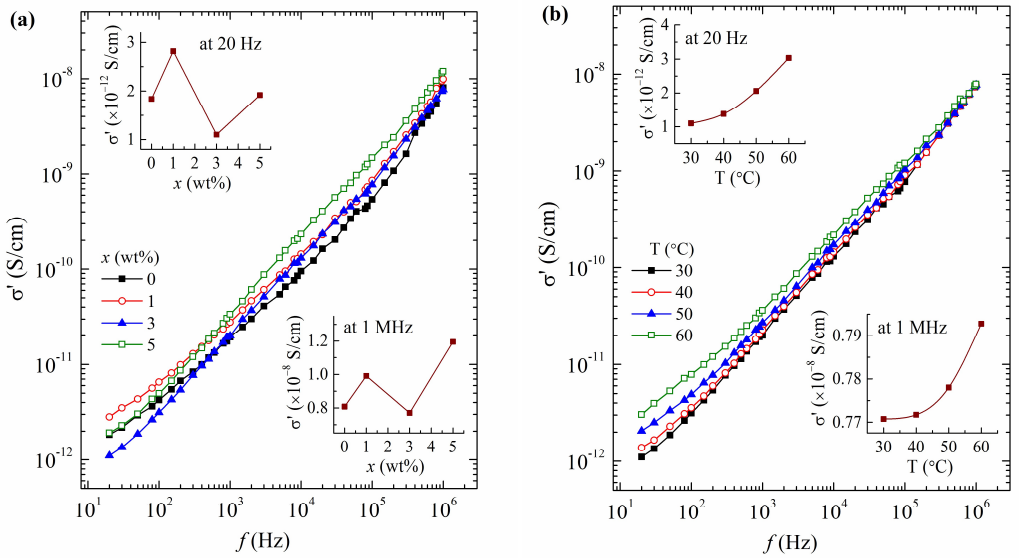

Fig. 7 — The spectra of real part σ′ of complex ac electrical conductivity of the (a) PVP–*x* wt% SiO_2 films for *x* values 0, 1, 3 and 5 at 30 °C, and (b) PVP–3 wt% SiO_2 film at temperatures 30, 40, 50, and 60 °C. The insets show the values of σ′ at 20 Hz and 1 MHz.

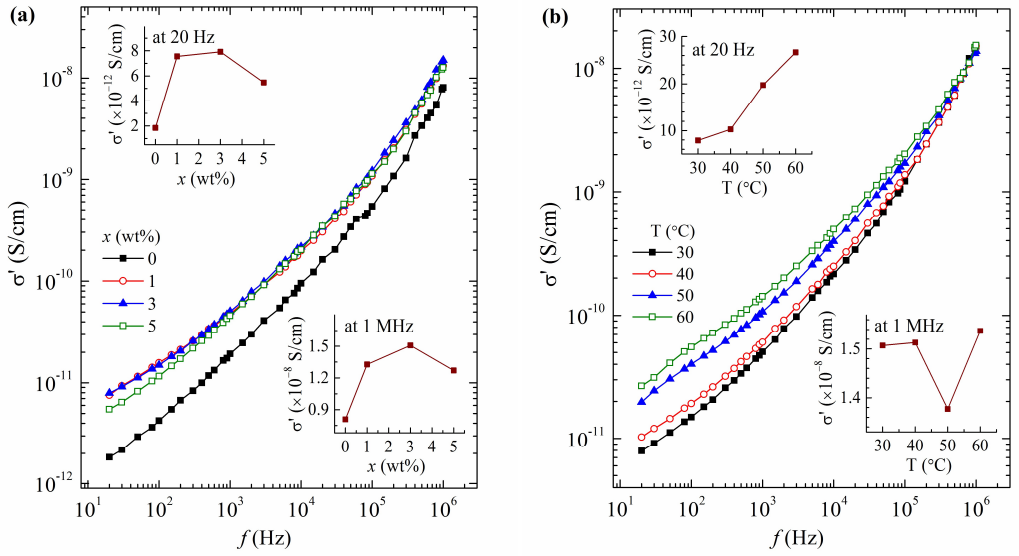

Fig. 8 — The spectra of real part σ′ of complex ac electrical conductivity of the (a) PVP–*x* wt% Al_2O_3 films for *x* values 0, 1, 3 and 5 at 30 °C, and (b) PVP–3 wt% Al_2O_3 film at temperatures 30, 40, 50, and 60 °C. The insets show the values of σ′ at 20 Hz and 1 MHz.

the increase of temperature of the PNC film confirming the thermally activated behaviour of this relaxation process. In the case of 5 wt% SiO_2 containing PNC film a broad and diffused hump can be seen in the intermediate frequency range of M'' spectra (Fig. 5a) which could be assigned to the relaxation process of the pyrrolidone ring of the PVP repeat units.

Electrical conductivity spectra

The alternating current (ac) electrical conductivity (real σ′) spectra of the PVP–*x* wt% SiO_2 films and PVP–*x* wt% Al_2O_3 films are presented in Figs. 7 and 8, respectively. It can be noted from Fig. 7 that the σ′ increase non-linearly with the increase of frequency for the SiO_2 containing PNC films but the non-linearity is more pronounced for the Al_2O_3 containing PNC films (see Fig. 8). The non-linear variation of σ′(*f*) is commonly exhibited for the semicrystalline PNC materials[9,15,16], but the frequency dependent non-linear behaviour for these amorphous PNC materials is mainly due to heterogeneity in these materials. Further, it is can be read from the σ′ plots that there is about four orders of magnitude increase in σ′ with the increase in frequency by five orders of magnitude.

Furthermore, it is noted that the σ′ values at 20 Hz are of the order of 10^{-12} S/cm and at 1 MHz there are about 10^{-8} S/cm (plotted in insets of the figures). The low σ′ values confirm the high electric insulation ability of these hybrid nanocomposite materials.

The insets of Figs. 7 and 8 also reveal that the σ′ values at fixed frequency vary anomalously with the increase of nanofiller concentration but there is a non-linear increase in σ′ values with the increase of temperature of the 3 wt% nanofillers containing PNC films. Further, it is noted that the σ′ values at 1 MHz are almost independent of the film temperature which confirms that the electrical conduction is highly stabilized against temperature variation from 30 to 60 ºC at radio frequencies for these PNC films.

Conclusions

This manuscript reports the complex dielectric permittivity and ac electrical conductivity dispersion behaviour of the PVP–*x* wt% SiO_2 films and PVP–*x* wt% Al_2O_3 films in the frequency range 20 Hz to 1 MHz at a fixed temperature and also with the temperature variation for a fixed nanofiller concentration PNC films. All these PNC materials are highly amorphous mainly due to the amorphous nature of the host PVP matrix and also the SiO_2 nanofiller, and the low degree of crystallinity of Al_2O_3 nanofiller. The frequency dependent real part (ε′) of the complex dielectric permittivity of these PNC films of different SiO_2 and Al_2O_3 concentrations are found in the range 2.4 to 3.4 at lower frequencies (f < 1 kHz) and 2.3 to 2.9 at higher frequencies at 30°C. The ε″ and tanδ values of these PNC materials are also observed relatively high at low frequencies but at high frequencies, these are significantly small ≤0.05. Further, the ε′ and ε″ largely enhance at low frequencies with the increase of temperature of the films but the effect of temperature is found insignificant at higher frequencies. Therefore, these materials could be used as nanodielectric substrate for the development of biodegradable microelectronic devices and also the materials for energy storing devices. Further, the ac electrical conductivity of these materials is found reasonably low (~10^{-12} S/cm at 20 Hz and ~10^{-8} S/cm at 1MHz) which confirms the suitability of these hybrid materials as biodegradable insulators. At 30°C, the relaxation process was not observed in the modulus spectra but the 3 wt% Al_2O_3 containing PNC film exhibit the interfacial polarization relaxation process below 100 Hz at 50 and 60°C which is found a thermally activated process.

Acknowledgement

One of the authors (PD) appreciatively acknowledges the award of Postdoctoral Fellowship (Research Associate) by the Council of Scientific and Industrial Research (CSIR), New Delhi.

References

1 Tanaka T & Imai T, Advanced Nanodielectrics: Fundamentals and Applications. *Jenny Stanford Publishing*, (*New York*), 2017.
2 Shen Y, Zhang X, Lin Y & Nan C W, Polymer Nanocomposites Dielectrics for Energy Applications. in: Lin Z, Yang Y, Zhang A (Eds) Polymer-Engineered Nanostructures for Advanced Energy Applications. Engineering Materials and Processes. *Springer,* (*Cham, Switzerland*), 2017.
3 Guo J Z, Song K & Liu C, Polymer-Based Multifunctional Nanocomposites and their Applications. *Elsevier Inc*., (*Amsterdam*), 2019.
4 Lau K Y, Vaughan A S & Chen G, *IEEE Elect Insul Mag*, 31 (2015) 45.
5 Tan D Q, *Adv Funct Mater*, 30 (2019) 1808567.
6 Sanida A, Stavropoulos S G, Speliotis Th & Psarras G C, *Mater Today Proc*, 5 (2018) 27491.
7 Smith R C, Liang C, Landry M, Nelson J K & Schadler L S, *IEEE Trans Dielectr Electr Insul*, 15 (2008) 187.
8 Morsi M A, Rajeh A & Al-Muntaser A A, *Compos Part B*, 173 (2019) 106957.
9 Choudhary S & Sengwa R J, *Curr Appl Phys*, 18 (2018) 1041.
10 Choudhary S & Sengwa R J, *J Polym Res*, 24 (2017) 54.
11 S Choudhary, *Indian J Eng Mater Sci*, 23 (2016) 399.
12 Anandraj J & Joshi G M, *Compos Interfaces*, 25 (2018) 455.
13 Manika G C & Psarras G C, *Exp Polym Lett*, 13 (2019) 749.
14 Ambrosio R, Carrillo A, Mota M L, de la Torre K, Torrealba R, Moreno M, Vazquez H, Flores J & Vivaldo I, *Polymers*, 10 (2018) 1370.
15 Sengwa R J, Choudhary S & Dhatarwal P, *J Mater Sci Mater Electron*, 30 (2019) 12275.
16 Sengwa R J, Choudhary S & Sankhla S, *Compos Sci Technol*, 70 (2010) 1621.
17 Sengwa R J & Choudhary S, *Polym Bull*, 72 (2015) 2591.
18 Dhatarwal P & Sengwa R J, *J Polym Res*, 26 (2019) 196.
19 Wu Z, Wang T, Sun C, Liu P, Xia B, Zhang J, Liu Y & Gao D, *AIP Adv*, 7 (2017) 125213.
20 Divyasree M C, Shiju E, Francis J, Anusha P T, Rao S V & Chandrasekharan K, *Mater Chem Phys*, 197 (2017) 208.
21 Cao W, Zhou P, Liao Y, Yang X, Pan D, Li Y, Pang B, Zhou L & Su Z, *Sensors*, 19 (2019) 2077.
22 Hsiao C N & Huang K S, *J Appl Polym Sci*, 96 (2005) 1936.
23 Chen S, Cheng B & Ding C, *J Macromol Sci*, 54 (2015) 481.
24 Mallakpour S & Sadeghzadeh R, *Polym Plastic Technol Eng*, 56 (2017) 1866.
25 Choudhary S & Sengwa R J, *J Inorg Organomet Polym Mater*, 29 (2019) 592.

26 Kochi R, Crasta V, Kumar R & Shetty G, *AIP Conf Proc*, 2100 (2019) 020045.
27 Abdelghany A M, Abdelrazek E M, Badr S I & Morsi M A, *Mater Design*, 97 (2016) 532.
28 Sengwa R J & Choudhary S, *J Appl Polym Sci*, 131 (2014) 40617.
29 Safo I A, Werheid M, Dosche C & Oezaslan M, *Nanoscale Adv*, 1 (2019) 3095.
30 Eskandari M, Ahmadi V & Ahmadi Sh, *Physica B*, 404 (2009) 1924.
31 Saravanan L, Diwakar S, Mohankumar R, Pandurangan A & Jayavel R, *Nanometer Nanotechnol*, 1 (2011) 42.
32 Ghosh G, Naskar M K, Patra A & Chatterjee M, *Optical Mater*, 28 (2006) 1047.
33 Gupta R K, Kennel E & Kim K J, Polymer Nanocomposites Handbook. *CRC Press*, (*Boca Raton*), 2009.
34 Alhabill F N, Ayoob R, Andritsch T & Vaughan A S, *Mater Design*, 158 (2018) 62.
35 Kumar S, Supriya S & Kar M, *Compos Sci Technol*, 157 (2018) 48.
36 Tsonos C, Zois H, Kanapitsas A, Soin N, Siores E, Peppas G D, Pyrgioti E C, Sanida A, Stavropoulos S G & Psarras G C, *J Phys Chem Solids*, 129 (2019) 378.
37 Halder M, Das A K & Meikap A K, *Mater Res Bull*, 104 (2018) 179.
38 Choudhary S, *Indian J Chem Technol*, 25 (2018) 51.
39 Luo Y, Wu G, Liu J, Peng J, Zhu G & Gao G, *IEEE Trans Dielect Electric Insul*, 21 (2014) 1824.
40 Sengwa R J, Choudhary S & Dhatarwal P, *Adv Compos Hybrid Mater*, 2 (2019) 162.
41 Sengwa R J & Choudhary S, *J Alloys Compd*, 701 (2017) 652.
42 Mallakpour S & Khadem E, *Prog Polym Sci*, 51 (2015) 74.
43 Choudhary S, *Polym Compos*, 39 (2018) E1788.
44 Sengwa R J & Choudhary S, *Adv Mater Proc*, 2 (2017) 280.
45 Yang Y, He J, Wu G & Hu J, *Sci Rep*, 5 (2015) 16986.
46 Saleh M, Al-Hajri Z, Popelka A & Zaidi S J, *Materials*, 13 (2020) 250.
47 Latief F H, Chafidz A, Junaedi H, Alfozan A & Khan R, *Adv Polym Technol*, 2019 (2019) 5173537.
48 Tański T, Matysiak W & Zaborowska M, *Arch Metall Mater*, 63 (2018) 211.
49 Kumar M S & Rao M C, *Heliyon*, 5 (2019) e02727.
50 Deshmukh K, Ahamed M B, Sadasivuni K K, Ponnamma D, Al-Ali AlMaadeed M, Deshmukh R R, Pasha S K K, Polu A R & Chidambaram K, *J Appl Polym Sci*, 134 (2017) 44427.
51 Xu F, Zhang H, Jin L, Li Y, Li J, Gan G, Wei M, Li M & Liao Y, *J Mater Sci*, 53 (2018) 2638.
52 Rajesh K, Crasta V, Rithin Kumar N B, Shetty G & Rekha P D, *J Polym Res*, 26 (2019) 99.
53 Mao F, Shi Z, Wang J, Zhang C, Yang C & Huang M, *Adv Compos Hybrid Mater*, 1 (2018) 548.